Received: 18 January 2021 | Accepted: 20 July 2021

DOI: 10.1002/bab.2227

WILEY

ORIGINAL ARTICLE

Detection of cholera toxin with surface plasmon field-enhanced fluorescent spectroscopy

Sebnem Seherler[1] | **Anil Bozdogan**[2,3] | **Tugba Arzu Ozal Ildeniz**[4] | **Fatma Nese Kok**[1] | **Ilke Anac Sakir**[2,5]

[1] Molecular Biology-Genetics and Biotechnology Programme, Istanbul Technical University, Istanbul, Turkey

[2] Department of Material Science and Engineering, Gebze Technical University, Kocaeli, Turkey

[3] Center for Electrochemical Surface Technology (CEST), Austrian Institute of Technology, Tulln, Austria

[4] Department of Medical Engineering, Faculty of Engineering, Acibadem Mehmet Ali Aydinlar University, Istanbul, Turkey

[5] Institute of Biotechnology, Gebze Technical University, Kocaeli, Turkey

Correspondence
Ilke Anac Sakir, Department of Material Science and Engineering, Gebze Technical University, Kocaeli, Turkey.
Email: ilkeanac@gtu.edu.tr

Funding information
Scientific and Technological Research Council of Turkey (TUBITAK), Grant/Award Number: 115E015

Abstract

In this work, a biosensor based on surface plasmon field-enhanced florescence spectroscopy (SPFS) method was successfully constructed to detect the truncated form of cholera toxin, that is, its beta subunit (CTX-B). CTX-B is a relatively small molecule (12 kDa) and it was chosen as model analyte for the detection of protein toxins originated from waterborne pathogens. Recognition layer was prepared on gold-coated LaSFN9 glasses modified with 11-mercaptoundecanoic acid (11-MUA). Biotin-conjugated anti-CTX-B polyclonal antibody (B-Ab) was immobilized on streptavidin (SA) layer constructed on the 11-MUA-modified surface. CTX-B amount was determined with direct assay using B-Ab in surface plasmon resonance (SPR) mode and with sandwich assay in SPFS mode using Cy5-conjugated anti-CTX-B polyclonal antibody. Minimum detected CTX-B concentrations were 10 and 0.01 μg/ml with SPR and SPFS, respectively, showing the sensitivity of the SPFS system over the conventional one. The detection was done in 2–6 h, which was faster than both culture and polymerase chain reaction (PCR)-based methods. Stability tests were performed with SA-coated sensors (excluding B-Ab). In this form, the layer was stable after 30 days of storage in phosphate-buffered saline (PBS; 0.01 M, pH = 7.4) at +4°C. B-Ab layer was formed immediately on them before each measurement.

KEYWORDS

antibody, biosensor, cholera toxin, environmental biotechnology, immobilization, surface plasmon resonance (SPR), surface plasmon field-enhanced fluorescent spectroscopy (SPFS)

1 | INTRODUCTION

Waterborne diseases caused by chemicals, bacteria, and viruses are estimated to cause more than 2 million deaths annually.[1,2] It is crucial to control diseases and epidemics generated by pathogens in drinking water supplies, as they not only cause deaths but also lead to important economic and labor losses. Bacteria associated with waterborne

Abbreviations: 11-MUA, 11-mercaptoundecanoic acid; B-Ab, biotinylated anti-cholera toxin antibody; CTX, cholera toxin; CTX-A, cholera toxin A subunit; CTX-B, cholera toxin B subunit; Cy5-Ab, Cy5-conjugated anti-cholera toxin antibody; EDC, n-(3-dimethylaminopropyl)-n′-ethyl carbodiimide; NHS, n-hydroxy succinimide; PBS, phosphate-buffered saline; PCR, polymerase chain reaction; SA, streptavidin; SP, surface plasmon; SPFS, surface plasmon field-enhanced fluorescent spectroscopy; SPR, surface plasmon resonance.

diseases include *Escherichia coli* O157:H7, *Salmonella* spp., *Salmonella typhi*, *Brucella* spp., *Shigella* spp., *Campylobacter* spp., *Pseudomonas* spp., *Vibrio cholerae*.[3] Cholera, a diarrheal disease caused by *V. cholerae* is estimated to affect 1.3–4 million people worldwide, and result in 21,000 to 143,000 deaths yearly. The number of cholera cases is very low in developed countries, while it is widespread in areas affected with natural disasters, floods, scarcity, and war.[4,5]

Cholera toxin (CTX) is a protein that is secreted from pathogenic strains of *V. cholerae*. CTX has A (28 kDa) and B (11.6 kDa) subunits assembled in AB_5 form. While A subunit (CTX-A) provides toxic activity, B (CTX-B) subunit is the pentameric nontoxic part that is responsible for the specific binding to its target.[6]

Culture-dependent methods are extensively used for the detection of the waterborne pathogens.[7–9] However, these methods are time consuming and often misleading as false negative results may be obtained due to existence of viable but not culturable strains. Culture-based detection of *V. Cholerae*, for example, requires bacterial growth in a liquid enrichment medium, a highly selective agar medium, and a less selective culture medium, which extends the analysis time to 2–8 days. To overcome these problems, molecular methods based on quantitative polymerase chain reaction (q-PCR),[10–12] multiplex PCR,[13,14] microarrays,[15–17] biosensors,[18–20] and immunoassays[21,22] have been developed for the detection of pathogens. Among these methods, immunoassay-based methods require pre-enrichment to reduce the cell surface antigens, while DNA extraction and post-amplification processes are needed in PCR-based detection of pathogens.[23] In order to decrease the pretreatment steps and detection time, different label-free biosensors such as electrochemical impedance spectroscopy,[24,25] fiber optics,[26] and surface plasmon resonance (SPR)[27] were successfully developed as an alternative to immunoassays and PCR-based techniques.[28,29]

Biosensors developed for the detection of *V. cholerae* are based on three analyte types: whole cells, nucleic acids, and toxins. *V. cholerae* O1 cells were detected via SPR[30] and atomic force microscopy[31] based biosensors using surface protein-specific antibodies, whereas ctxA DNA was detected using microcantilever sensor[32] and electrochemical biosensors utilizing various complex designs including composite nanoparticles[33] and microspheres.[34]

SPR has been extensively used for the detection and interaction of proteins, nucleic acids, lipids, carbohydrates, and cells.[35–37] These biosensors provide faster and simpler analysis of bacterial pathogens compared to the culture, PCR, and immune-absorbent assays.[38,39] SPR-based biosensors have been recently developed for the detection of *V. cholerae*,[30] *S. enterica*,[40] and *P. fijiensis*.[41] These biosensors are attractive, as they provide label-free detection of analytes in real-time through refractive index changes. These changes enable the direct observation of large- and medium-size molecules as larger the molecules, higher the refractive index changes. However, the detection of very low analyte concentrations and small molecules is a challenge for SPR biosensors.[42] Various attempts have been made to increase the resolution of RI change and lower the detection limit of SPR biosensors via interface designs and signal enhancements based on plasmonic and non-plasmonic nanoparticles.[43]

Surface plasmon field-enhanced fluorescence spectroscopy (SPFS) was proposed by Liebermann and Knoll[44] in order to increase the sensitivity of SPR. In SPFS method, surface plasmons (SPs) generated at the metal surface enhance the fluorescence signal of the fluorophores in the vicinity of the surface. This enhancement is achieved when the SPs are excited at the absorption wavelength of fluorophore label.[45] Highest fluorescence signal is obtained when the absorption is coupled to the SP modes. Fluorescence intensity peak position is slightly displaced from SPR angle, because SP waves interfere with directly reflected laser beams. Coupling of SPs to the fluorescence excitation results in orders of magnitudes of higher excitation.[42,44]

SPFS was previously used for the detection of various biomolecular interactions including DNA/DNA hybridization,[46,47] peptide nucleic acid (PNA)/DNA hybridizations,[48] proteins such as prostate-specific antigen (prostate cancer biomarker),[49,50] vesicle fusion studies,[51] influenza virus,[52] and membrane protein expression.[53] Recently, SPFS has been used for detection of biomolecules with antibody-based (in sandwich assay format)[54] and aptamer-based[55] capture elements. To the best of our knowledge, the detection of waterborne pathogen toxins using SPFS has not been reported in the literature before.

In this study, SPFS was used, for the first time, to detect the CTX-B subunit, which is a truncated form of waterborne pathogen toxin and a relatively small molecule (12 kDa). First, gold-coated SPR surfaces were functionalized with 11-mercaptoundecanoic acid (11-MUA) to create a self-assembled monolayer. Streptavidin (SA)-biotinylated anti-cholera toxin beta polyclonal antibody (B-Ab) complex was then immobilized on 11-MUA layer as the recognition unit. This recognition layer was used in direct detection of CTX-B in SPR mode. For SPFS studies, Cy5-conjugated anti-cholera toxin beta polyclonal antibody (Cy5-Ab) was used as the second antibody for sandwich assay format. Cy5 dye is a far-red fluorescence-emitting dye that is used in many biological applications, with excitation/emission wavelengths at 625, 650, and 670 nm. Cy5 dye was chosen to match the wavelength of light emitted from He/Ne laser (632.8 nm).

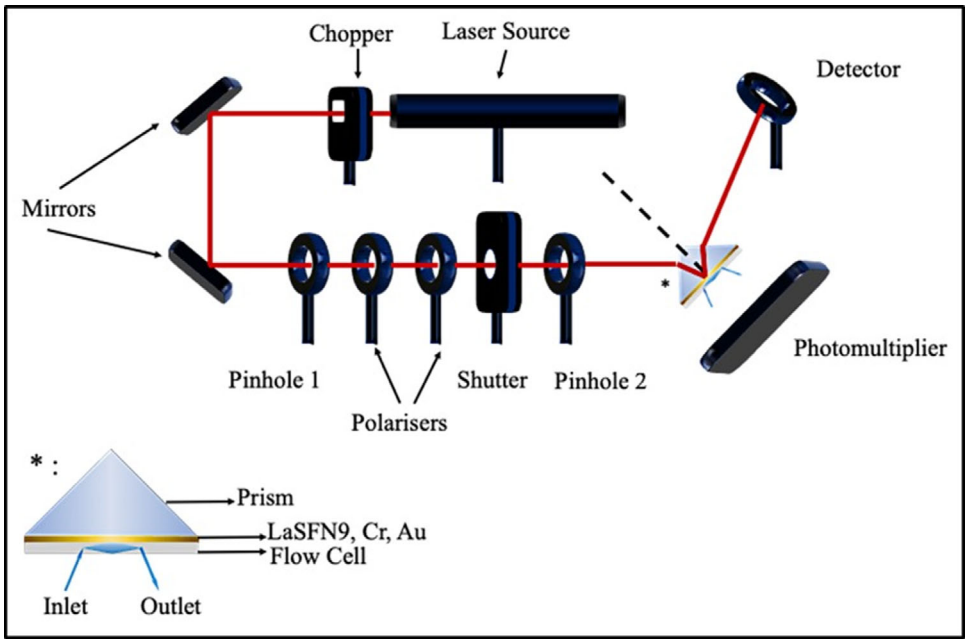

FIGURE 1 Instrumental setup of SPR/SPFS system. Photomultiplier and shutter were mounted only for fluorescence measurement. "*" indicates sample holder (not in scale)

2 | MATERIALS AND METHODS

2.1 | Materials

CTX beta subunit (CTX-B; C9903), SA (9013-20-1), 11-MUA (71310-21-9), n-hydroxy succinimide (NHS; 6066-82-6), n-(3-dimethylaminopropyl)-n′-ethyl carbodiimide (EDC; 1892-57-5), MES (4432-31-9), phosphate-buffered saline (PBS; P4417) tablets, and ethanol were purchased from Sigma-Aldrich. Biotin-conjugated CTX-B polyclonal antibody (B-Ab; PA1-73190) was purchased from ThermoFisher Scientific and Cy5-Ab (bs-12862R-Cy5) was purchased from Bioss Antibodies.

PBS and MES buffers were filtered through 0.2-μm filters. CTX-B, SA, and antibodies were aliquoted and stored at −20°C. NHS was stored as aliquots in MES buffer, while EDC was freshly prepared before each use.

2.2 | Instruments and measurements

The measurements were performed with SPFS (RESTEC 2005). The SPSF setup for the measurements is given in Figure 1. The monochromatic light emitted from HeNe laser (632.8 nm, [Uniphase], monochromatic, linear, transverse magnetic [TM, p] polarization [Glan-Thompson polarizer, B, Hale]) first passes through the chopper that is connected to the lock-in amplifier. After being reflected from two mirrors, the incident light passes through first pinhole and reaches the two successive polarizers. First polarizer is employed to adjust the light intensity and the second one is used for p-polarization. p-Polarized light then passes through a second pinhole and reaches the sample holder (Figure 1 - inset) containing a right-angle prism (n = 1.85) in Kretschmann configuration, sample and the flow cell. Sample holder is placed on a two-cycle goniometer (resolution of 0.05°, Huber). The reflected light is collected via BPW 24 B silicon photodiode. For the SPFS measurements, shutter was placed between the second polarizer and the second pinhole. Fluorescence module—composed of lens, band-pass filter, and photomultiplier—is mounted behind the flow cell.

In the angular scan mode, the system sweeps given angular interval and records the reflected intensity. In this study, angular scans were measured between 20° and 45° for air and between 40° and 65° for aqueous environments. In the kinetic mode, measurements were performed at a fixed angle corresponding 30% reflectivity achieved from the angular scan. The whole optical system was contained in a black box to avoid interference of the ambient light with the fluorescence signal.

2.3 | Preparation of recognition layer and SPFS measurement

2.3.1 | Activation of slide surface

LaSFN9 glass slides (n = 1.8449) (25.4 × 25.4 × 1.5 mm) were coated with 2-nm chromium and 50-nm gold using

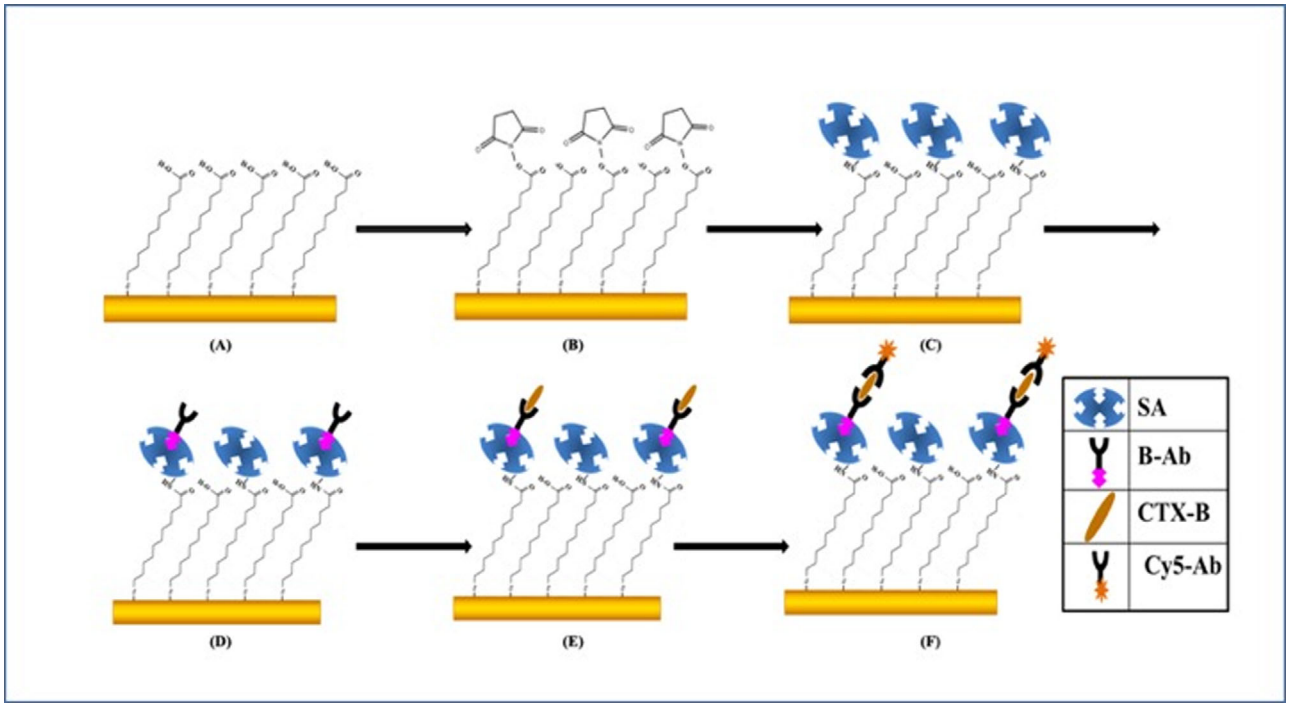

FIGURE 2 Surface functionalization and assay format. (A) 11-Mercaptoundecanoic acid SAM formation. (B) EDC/NHS activation. (C) Streptavidin binding. (D) Biotinylated antibody binding. (E) CTX-B binding. (F) Cy5-Ab binding in SPFS mode

a Nanovak NVTE4-01 thermal evaporator. The slides were immersed in 1 mM 11-MUA in ethanol overnight to allow self-assembled monolayer formation (Figure 2A). The slides were then washed three times with ethanol and steam-dried with N2.[56] 11-MUA-coated LaSFN9 slides were placed onto the PDMS flow cell as indicated in Figure 1 (inset). Index matching oil (n = 1.7, Cargille) was used between the SPR slide and the high-index right-angle prism. A peristaltic pump with tygon tubing was used for the control of liquid flow with the flow rate of 1.3 ml/min.

2.3.2 | Immobilization of antibodies

11-MUA-coated slides were first hydrated with PBS buffer (pH 7.4), then activated using 1:1 mixture of EDC (0.4 M):NHS (0.1 M) in MES buffer (pH 6) for 10 min (Figure 2B). Following the activation, SA (0.02–0.05 mg/ml) was immobilized on the surface (Figure 2C). Recognition layer was completed after the immobilization of B-Ab (0.05 mg/ml, 1:100 dilution) (Figure 2D). The reactions were followed in the kinetic mode, and after binding reactions were completed, unbound molecules were washed off with PBS buffer and then an angular scan was taken.

2.3.3 | CTX-B detection

Various concentrations of CTX-B (10 ng/ml to 20 μg/ml) were used to determine the working range of the biosensor (Figure 2E). Fluorescence measurements were performed via sandwich assay by injection of Cy5-Ab (1:5000 dilution) (Figure 2F).

2.4 | Stability tests

For the storage stability test, SA-coated surfaces were immersed in 50-ml PBS buffer (pH 7.4) in Hellendahl staining jar at +4°C. PBS solution was changed every 7 days. On day 30, the slide surfaces were washed and mounted to the sample holder. Reflectivity changes upon CTX-B binding for day 0 and day 30 were compared.

3 | RESULTS AND DISCUSSIONS

Self-assembled monolayers (SAMs) are used extensively to modify the interfaces between a transducer and a liquid sample. Alkane thiol SAMs are especially preferred to attach biomolecules to metal surfaces by His-Tag, SA-biotin-based binding, and amine coupling.[45] In this study, 11-MUA was used to generate the alkane thiol SAM. The angular scans of the 11-MUA layer in air and in buffer (Figure S1) were taken before the EDC/NHS activation. The angle corresponding to 30% of the reflectivity of the angular scan in buffer was taken as the kinetic angle (typically around 55°–57°). This angle was kept constant in kinetic measurements for all binding events for each experimental

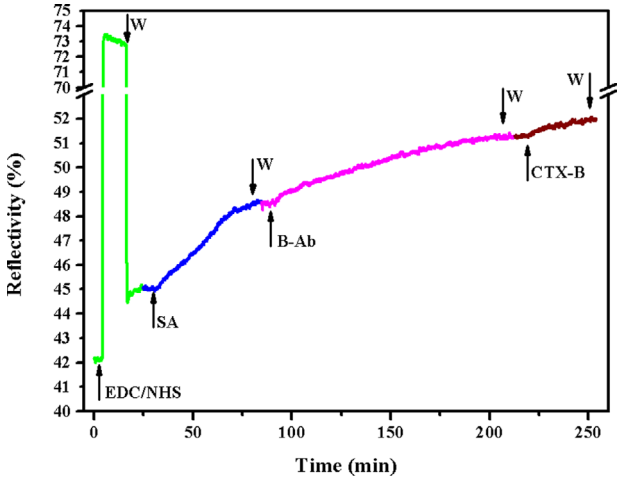

FIGURE 3 Label-free detection of CTX-B at pH 7.4. 11-Mercaptoundecanoic (11-MUA) surface was activated (green) with 1:1 mixture of EDC (0.4 M):NHS (0.1 M) in MES buffer (pH 6). SA, streptavidin (0.05 mg/ml, blue); B-Ab, biotinylated CTX-B antibody (0.05 mg/ml, purple); W, washing step. CTX-B (10 μg/ml, brown)

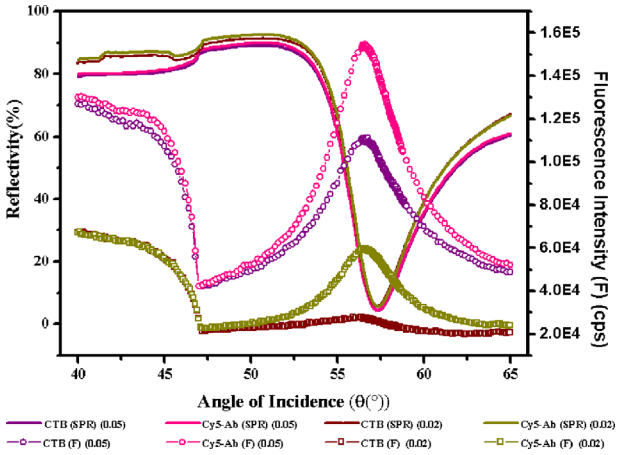

FIGURE 4 Effect of SA concetration on fluorescence intensity. CTX-B and Cy5-Ab concentrations were 0.1 μg/ml and 1:5000 dilution, respectively. Solid lines indicate angular scan, and open markers indicate fluorescent intensity. Open circles: 0.02 mg/ml SA; open squares: 0.05 mg/ml SA

set. EDC-NHS activation, SA, and capture antibody (B-Ab) bindings were kinetically observed without fluorescence on SPR mode (direct assay). After each layer formation, an angular scan was taken to compare reflectivity changes.

The kinetic scan of the binding events and label-free detection of CTX-B in different pH conditions are shown in Figure S2. The label-free detection of CTX-B was carried out in pH 7.4, because the binding signal was more resolved and washing step (W) did not affect the signal, indicating a strong binding event at pH 7.4 (Figure 3).

For SPFS measurements, the effect of SA concentration on CTX-B detection was studied in two different SA concentrations (0.02 and 0.05 mg/ml). Both detections were performed using 0.1 μg/ml CTX-B. While the SPR angle is slightly higher for higher SA concentration (0.05 mg/ml), SPR angle shift after Cy5-Ab binding was indistinguishable for both cases (Figure 4 - solid lines). When the fluorescence intensities (F) were compared, the background fluorescence was higher for 0.05 mg/ml SA. As this background fluorescence affects the signal-to-noise ratio and hence the sensitivity, SA concentration was reduced to 0.02 mg/ml for SPFS measurements.

Figure 5A,B shows the angular scan with reflectivity and fluorescent intensity changes and kinetic measurements of analyte detection at the optimal conditions for 0.01 μg/ml CTX-B (Figure 5). Angular scans in Figure 5A (solid lines) show that while CTX-B binding did not introduce any SPR angle shift, Cy5-Ab binding slightly shifted SPR angle toward higher values, indicating SPR alone does not provide a good resolution for direct analysis of toxin in lower concentrations. In addition to angular scans,

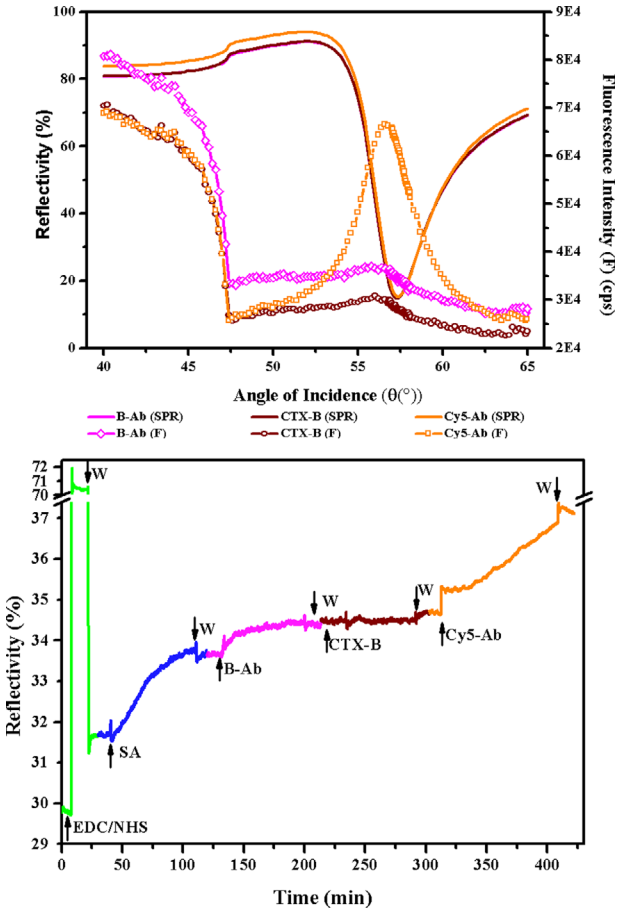

FIGURE 5 0.01 μg/ml CTX-B detection with SPR. Concentrations of CTX-B and Cy5-Ab were 0.01 μg/ml and 1:5000 dilution, respectively. (A) Angular scan with reflectivity and fluorescent intensity changes. (B) Kinetic measurements

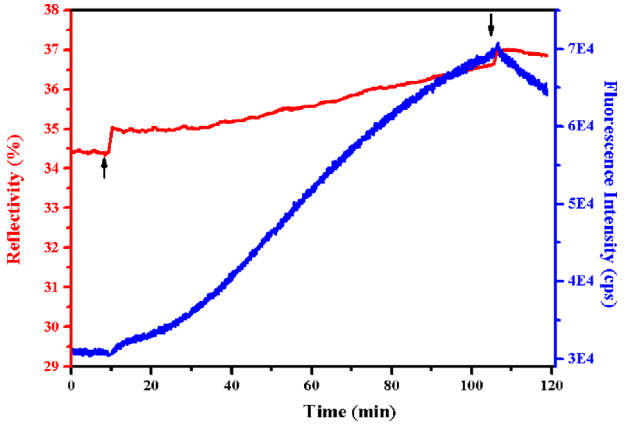

FIGURE 6 0.01 μg/ml CTX-B detection with SPFS. Reflectivity (red) and flourescent intensity (blue) changes upon Cy5-Ab binding

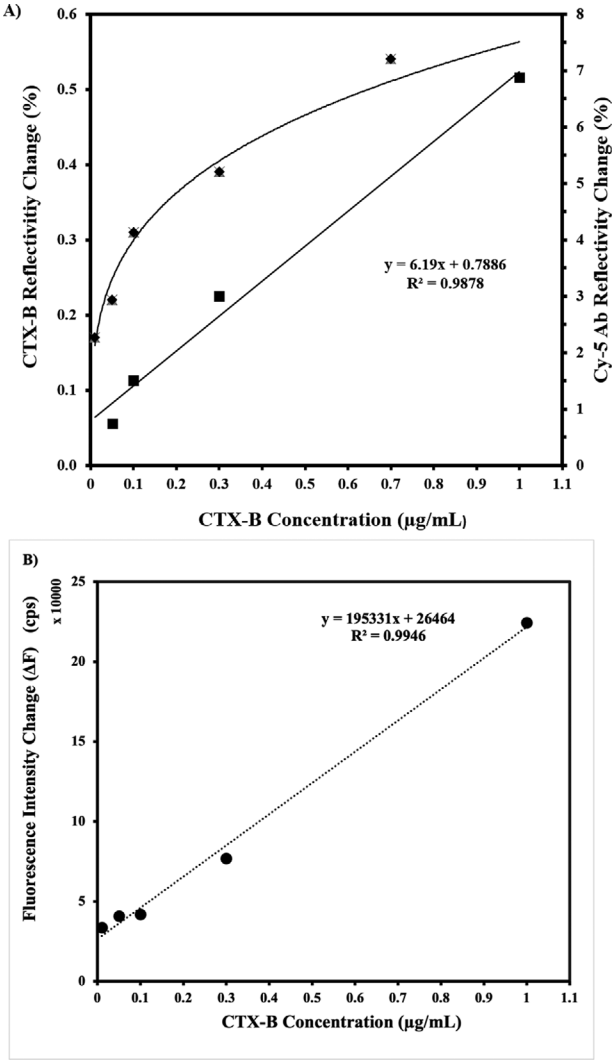

FIGURE 7 CTX-B detection range. (A) Reflectivity change after CTX-B (◆) and Cy5-Ab (■) binding. (B) Fluorescence intensity change after Cy5-Ab (●) binding

fluorescence intensities associated with the binding of B-Ab, CTX-B, and Cy5-Ab are shown in Figure 5A. Fluorescence intensity signal of Cy5-Ab was significantly higher from the background signals of B-Ab and CTX-B. Time-resolved kinetic analysis of this measurement is shown in Figure 5B beginning with the activation of 11-MUA surface. The total time required for surface preparation and detection was ca. 400 min, while detection time (binding of CTX-B and then Cy5-Ab) was 150 min. While the binding of SA, B-Ab, and Cy5-Ab increases the reflectivity (hence the SPR angle), CTX-B binding in this concentration did not cause a distinguishable reflectivity change. Cy5-Ab binding to CTX-B was followed both by SPR reflectivity change and SPFS fluorescence intensity change in the kinetic mode (Figure 6). The reflectivity change upon Cy5-Ab binding was 2.44% in SPR mode while in SPFS mode, a 108.92% increase in fluorescence signal was detected corresponding to 33,675 cps, which provides better resolution for CTX-B detection. High fluorescence signal in SPFS mode compared to almost undetectable/low-reflectivity change in SPR mode can also be observed for different measurements (Figure S3).

The linear working range of the biosensor was determined between 0.01 and 1 μg/ml concentrations of CTX-B (Figure 7). A linear response cannot be obtained with direct CTX-B detection, whereas the sandwich assay involving Cy5-Ab binding improved the sensor performance and results in linear relation with $R^2 = 0.9878$ in SPR mode (Figure 7A). A higher linear correlation ($R^2 = 0.9946$) was obtained when the fluorescence intensity was followed by SPFS indicating its advantage over SPR (Figure 7B). According to the Center for Disease Control and Prevention (CDC) guidelines, commonly used *V. cholerae* detection assays typically detect the toxin between 10 pg and 500 ng range.[57] In addition, the lethal concentration of CTX is 0.1 μg/ml (100 ng/ml).[58] The LOD of SPFS-based biosensor in this study is comparable with the commonly used methods and below the lethal concentration of CTX.

In order to determine the shelf life of the biosensor, surfaces were kept at +4°C for 30 days after the formation of SA layer. These surfaces were then used for the detection of 0.1 μg/ml CTX-B with both direct and Cy5-Ab-based detection. Relative reflectivity changes were calculated by assigning 100% activity to the day 0 samples. While 90% activity was retained with CTX-B detection, Cy5-Ab-based sensing was more sensitive to the storage conditions and activity was dropped to 75% (Figure 8).

Reproducibility of the biosensor was tested for 0.1 μg/ml CTX-B concentration. Standard deviation values were 23% (0.405 ± 0.095) and 7.3% (1.51 ± 0.11) for direct and Cy5-Ab-based detection in SPR mode. When Cy5-Ab fluorescence intensities were used in SPFS mode, standard deviation was determined as 11% (37,609 ± 4322) showing that

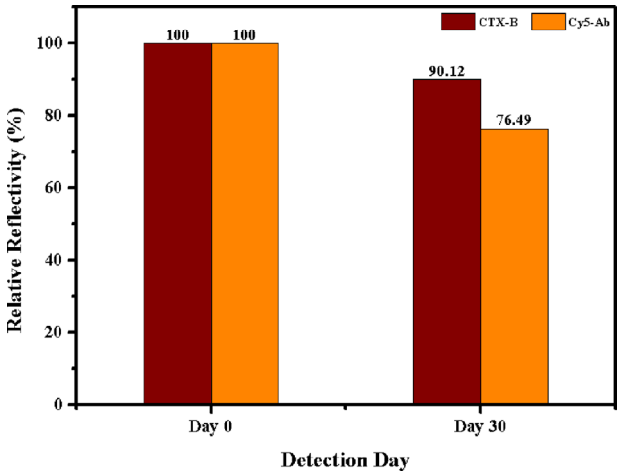

FIGURE 8 Stability of recognition layer. All samples were coated with 0.02 mg/ml streptavidin. CTX-B and Cy5-Ab concentrations were 0.1 μg/ml and 1:5000 dilution, respectively. Recognition layers were produced on day 0. CTX-B detection was performed at day 0 and day 30

reproducibility values were improved with the use of secondary antibody (Cy5-Ab) and SPFS.

Detection durations for CTX-B were calculated as time interval between the injection of CTX-B and the signal stabilization after Cy5-Ab binding. These detection times greatly differed depending on the CTX-B concentrations. CTX-B and Cy5-Ab binding signals were stabilized between 60 and 120 mins and 100 and 230 min, respectively, with increasing toxin concentration.

In the literature, CTX detection was done by several research groups using different detection techniques,[59–77] and either whole toxin (CTX, AB_5 form) or its truncated form (CTX-B) were used (Table S1). The commonly used capture molecules are anti-CTX-B antibodies and GM1 (binding target of CTX). When CTX, not the truncated form, was used, relatively lower detection limits (0.09 aM and 0.11 fM) were achieved with immunoassay and electrochemical immunosensor, respectively.[59,60] Different design strategies using different transducers have yielded in 0.1 pM to 10 nM LOD values.[61–67] When CTX-B was used as model analyte, 0.2–12 ng/ml LOD values were achieved by different groups,[68–74] which is the range of our LOD (10 ng/ml). Detection limits lower than 1 ng/ml were obtained either by complex detection protocols involving several steps[69] or by the use of home-made apparatus via magnetic frequency mixing detection.[71] Our system gave better results when compared to localized SPR (LSPR)-based system (LOD: 20 nM, 240 ng/ml) proposed by Bruzas et al.[75] Improved LOD values were obtained when affinity peptides were used against CTX-B (LOD: 3.51 ng/ml),[73] probably because of the usage of small molecules instead of large antibodies; as SPs have evanescent character, the distance of binding event from the surface is crucial and should be as low as possible.

4 | CONCLUSIONS

The presence of *V. cholerae* is determined by culture-dependent methods, PCR and biosensors on the whole cell, pathogenic organism DNA or protein toxin. In this study, we evaluated an SPFS-based biosensor for the detection of CTX-B in ng/ml level sensitivity. The obtained LOD value was within the range of commonly used CT detection methods listed in CDC guidelines and also lower than the lethal concentration of CT in human body. As the CTX-B subunit is relatively small molecule (12 kDa), the SPR angle shifts for lower concentrations were indistinguishable in the conventional SPR methodology. With the use of an additional fluorescence module to the SPR angular mode, the performance parameters of biosensor, namely detection limit, reproducibility values, linear range of detection were improved. The detection time (2–6 h depending on concentration) is significantly lower from both culture-(typically 2–8 days with multiple enrichment steps) and PCR-based detection (DNA extraction and postamplification steps) and comparable to immunoassays (3.5–18 h). In summary, a common sandwich assay design was used to emphasize the advantage of SPFS technique over SPR using shelf-ready agents. The sensitivity of the detection system could be further improved using higher affinity and/or smaller capture molecules. The biosensor system was not studied with complex water samples involving suspended solids. Pretreatment protocols for the water samples may vary according to the water source but for drinking water, which is our target sample, no pretreatment is needed. However, when working with drinking water, preconcentration step may be needed to detect even lower toxin levels. Thus, this biosensor can be used without any pretreatment to screen drinking water supplies, but for more complex samples containing suspended solids, a prefiltering step will be necessary.

ACKNOWLEDGMENT

The authors would like to thank the Scientific and Technological Research Council of Turkey (TUBİTAK) (Grant No: 115E015) for providing financial support to this project.

ORCID

Sebnem Seherler https://orcid.org/0000-0002-3554-4134
Fatma Nese Kok https://orcid.org/0000-0002-5093-6013
Ilke Anac Sakir https://orcid.org/0000-0001-8501-6455

REFERENCES

1. Diarrhoeal disease. World Health Organization; 2020. Available from: https://www.who.int/news-room/fact-sheets/detail/diarrhoeal-disease. Accessed on 3 August, 2021.
2. Foodborne and waterborne diseases. BC Centre for Disease Control; 2019. Available from:https://www.bccdc.ca/health-info/disease-types/foodborne-waterborne-diseases. Accessed on 3 August, 2021.
3. Girones R, Ferrús MA, Alonso JL, Rodriguez-Manzano J, Calgua B, de Abreu Corrêa A, et al. Molecular detection of pathogens in water–the pros and cons of molecular techniques. Water Res. 2010;44:4325–39.
4. World Health Organization. World Health Statistics 2018: Monitoring Health for the SDGs, Sustainable Development Goals. Geneva: World Health Organization; 2018.
5. Baldauf KJ, Royal JM, Hamorsky KT, Matoba N. Cholera toxin B: one subunit with many pharmaceutical applications. Toxins. 2015;7:974–96.
6. Sanchez J, Holmgren J. Cholera toxin - a foe & a friend. Indian J Med Res. 2011;133(2):153–63.
7. Wu J, Stewart JR, Sobsey MD, Cormency C, Fisher MB, Bartram JK. Rapid detection of escherichia coli in water using sample concentration and optimized enzymatic hydrolysis of chromogenic substrates. Curr Microbiol. 2018;75:827–34.
8. Ngwa GA, Schop R, Weir S, León-Velarde CG, Odumeru JA. Detection and enumeration of E. coli O157:H7 in water samples by culture and molecular methods. J Microbiol Methods. 2013;92:164–72.
9. Oliver JD, Corry JEL, Curtis GDW, Baird RM, editors. Handbook of culture media for food and water microbiology. 3rd ed. Royal Society of Chemistry; 2012. p. 377–402.
10. Botes M, de Kwaadsteniet M, Cloete TE. Application of quantitative PCR for the detection of microorganisms in water. Anal Bioanal Chem. 2013;405:91–108.
11. Kasturi KN, Drgon T. Real-time PCR method for detection of *Salmonella* spp. in environmental samples. Appl Environ Microbiol. 2017;83(14):1–12.
12. Yuan Y, Zheng G, Lin M, Mustapha A. Detection of viable *Escherichia coli* in environmental water using combined propidium monoazide staining and quantitative PCR. Water Res. 2018;145:398–407.
13. Molina F, López-Acedo E, Tabla R, Roa I, Gómez A, Rebollo JE. Improved detection of Escherichia coli and coliform bacteria by multiplex PCR. BMC Biotechnol. 2015;15:48.
14. Kim H-J, Ryu J-O, Lee S-Y, Kim E-S, Kim H-Y. Multiplex PCR for detection of the Vibrio genus and five pathogenic Vibrio species with primer sets designed using comparative genomics Applied microbiology. BMC Microbiol. 2015;15:1–11. https://doi.org/10.1186/s12866-015-0577-3
15. Gomes M, Vieira H, Vale FF. Characterization, validation and application of a DNA microarray for the detection of mandatory and other waterborne pathogens. J Biochem. 2015;158(5):393–401.
16. Shin HH, Seo JH, Kim CS, Hwang BH, Cha HJ. Hybrid microarray based on double biomolecular markers of DNA and carbohydrate for simultaneous genotypic and phenotypic detection of cholera toxin-producing *Vibrio cholerae*. Biosens Bioelectron. 2016;79:398–405.
17. Baudart J, Guillebault D, Mielke E, Meyer T, Tandon N, Fischer S, et al. Microarray (phylochip) analysis of freshwater pathogens at several sites along the Northern German coast transecting both estuarine and freshwaters. Appl Microbiol Biotechnol. 2016;101:871–86.
18. Zhao YW, Wang HX, Jia GC, Li Z. Application of aptamer-based biosensor for rapid detection of pathogenic *Escherichia coli*. Sensors (Basel). 2018;18:2518. https://doi.org/10.3390/s18082518
19. Kumar N, Hu Y, Singh S, Mizaikoff B. Emerging biosensor platforms for the assessment of water-borne pathogens. Analyst. 2018;143:359–73.
20. Silva NFD, Magalhães JMCS, Freire C, Delerue-Matos C. Electrochemical biosensors for Salmonella: State of the art and challenges in food safety assessment. Biosens Bioelectron. 2018;99:667–82.
21. Wu TF, Chen YC, Wang WC, Kucknoor AS, Lin CJ, Lo YH, et al. Rapid waterborne pathogen detection with mobile electronics. Sensors (Basel). 2017;17:1–11. https://doi.org/10.3390/s17061348
22. Han Y, Wu H, Cheng G, Zhe J. A two-stage microresistive pulse immunosensor for pathogen detection. Lab Chip. 2016;16:773–9.
23. Ramírez-Castillo FY, Loera-Muro A, Jacques M, Garneau P, Avelar-González FJ, Harel J, et al. Waterborne pathogens: detection methods and challenges. Pathogens. 2015;4:307–34.
24. Liu J, Jasim I, Abdullah A, Shen Z, Zhao L, El-Dweik M, et al. An integrated impedance biosensor platform for detection of pathogens in poultry products. Sci Rep. 2018;8:1–10.
25. Moghtader F, Congur G, Zareie HM, Erdem A, Piskin E. Impedimetric detection of pathogenic bacteria with bacteriophages using gold nanorod deposited graphite electrodes. RSC Adv. 2016;6:97832–9.
26. Abdelhaseib MU, Singh AK, Bailey M, Singh M, El-Khateib T, Bhunia AK. Fiber optic and light scattering sensors: complimentary approaches to rapid detection of Salmonella enterica in food samples. Food Control. 2016;61:135–45.
27. Homola J, Hegnerová K, Vala M. Surface plasmon resonance biosensors for detection of foodborne pathogens and toxins. In: Proc. SPIE 7167, Frontiers in Pathogen Detection: From Nanosensors to Systems, 716705. SPIE BIOS, San Jose, CA, USA (2009Feb 19).
28. de Dieu Habimana J, Ji J, Sun X. Minireview: trends in optical-based biosensors for point-of-care bacterial pathogen detection for food safety and clinical diagnostics. Anal Lett. 2018;51:2933–66.
29. Alahi MEE, Mukhopadhyay SC. Detection methodologies for pathogen and toxins: a review. Sensors (Basel). 2017;17:1885.
30. Taheri RA, Rezayan AH, Rahimi F, Mohammadnejad J, Kamali M. Development of an immunosensor using oriented immobilized anti-OmpW for sensitive detection of Vibrio cholerae by surface plasmon resonance. Biosens Bioelectron. 2016;86:484–8.
31. Sungkanak U, Sappat A, Wisitsoraat A, Promptmas C, Tuantranont A. Ultrasensitive detection of *Vibrio cholerae* O1 using microcantilever-based biosensor with dynamic force microscopy. Biosens Bioelectron. 2010;26:784–9.
32. Khemthongcharoen N, Wonglumsom W, Suppat A, Jaruwongrungsee K, Tuantranont A, Promptmas C. Piezoresistive microcantilever-based DNA sensor for sensitive detection of pathogenic Vibrio cholerae O1 in food sample. Biosens Bioelectron. 2014;63:347–53.

33. Rahman M, Heng LY, Futra D, Ling TL. Ultrasensitive biosensor for the detection of *Vibrio cholerae* DNA with polystyrene-co-acrylic acid composite nanospheres. Nanoscale Res Lett. 2017;12:1–12.
34. Low KF, Zain ZM, Yean CY. A signal-amplified electrochemical DNA biosensor incorporated with a colorimetric internal control for Vibrio cholerae detection using shelf-ready reagents. Biosens Bioelectron. 2017;87:256–63.
35. Wu Q, Sun Y, Zhang D, Li S, Zhang Y, Ma P, et al. Ultrasensitive magnetic field-assisted surface plasmon resonance immunoassay for human cardiac troponin I. Biosens Bioelectron. 2017;96:288–93.
36. Ashley J, D'Aurelio R, Piekarska M, Temblay J, Pleasants M, Trinh L, et al. Development of a β-lactoglobulin sensor based on SPR for milk allergens detection. Biosensors. 2018;8:1–11.
37. Huang CJ, Lin ZE, Yang YS, Chan HWH, Chen WY. Neutralized chimeric DNA probe for detection of single nucleotide polymorphism on surface plasmon resonance biosensor. Biosens Bioelectron. 2017;99:170–5.
38. Nguyen HH, Park J, Kang S, Kim M. Surface plasmon resonance: a versatile technique for biosensor applications. Sensors (Basel). 2015;15:10481–510.
39. Huang CJ, Knoll W, Sessitsch A, Dostalek J. SPR bacterial pathogen biosensor: the importance of fluidic conditions and probing depth. Talanta. 2014;122:166–71.
40. Wang B, Park B, Xu B, Kwon Y. Label-free biosensing of Salmonella enterica serovars at single-cell level J Nanobiotechnol. 2017;15:1–12. https://doi.org/10.1186/s12951-017-0273-6
41. Luna-Moreno D, Sánchez-Álvarez A, Islas-Flores I, Canto-Canche B, Carrillo-Pech M, Villarreal-Chiu JF, et al. Early detection of the fungal banana black sigatoka pathogen pseudocercospora fijiensis by an SPR immunosensor method. Sensors (Basel). 2019;19(3):1–12.
42. Dostálek J, Knoll W. Biosensors based on surface plasmon-enhanced fluorescence spectroscopy (review). Biointerphases. 2009;3(3):FD12–22.
43. Hinman SS, McKeating KS, Cheng Q. Surface plasmon resonance: material and interface design for universal accessibility. Anal Chem. 2019;90:19–39.
44. Liebermann T, Knoll W. Surface-plasmon field-enhanced fluorescence spectroscopy. Colloids Surf A. 2000;171:115–30.
45. Bauch M, Toma K, Toma M, Zhang Q, Dostalek J. Plasmon-enhanced fluorescence biosensors: a review. Plasmonics. 2014;9:781–99.
46. Neumann T, Johansson ML, Kambhampati D, Knoll W. Surface-plasmon fluorescence spectroscopy. Adv Funct Mater. 2002;12(9):575–86.
47. Tawa K, Knoll W. Mismatching base-pair dependence of the kinetics of DNA–DNA hybridization studied by surface plasmon fluorescence spectroscopy. Nucleic Acids Res. 2004;32(8):2372–7.
48. Park H, Germini A, Sforza S, Corradini R, Marchelli R, Knoll W. Kinetic and affinity analyses of hybridization reactions between peptide nucleic acid probes and DNA targets using surface plasmon field-enhanced fluorescence spectroscopy. Biointerphases. 2007;1(4):113–22.
49. Chang YF, Hung SH, Lee YJ, Chen RC, Su LC, Lai CS, et al. Discrimination of breast cancer by measuring prostate-specific antigen levels in women's serum. Anal Chem. 2011;83(13):5324–8.
50. Zhang Q, Wu L, Wong TI, Zhang J, Liu X, Zhou X, et al. Surface plasmon-enhanced fluorescence on Au nanohole array for prostate-specific antigen detection. Int J Nanomedicine. 2017;12:2307–14.
51. Morigaki K, Tawa K. Vesicle fusion studied by surface plasmon resonance and surface plasmon fluorescence spectroscopy. Biophys J. 2006;91(4):1380–7.
52. Nomura KI, Gopinath SCB, Lakshmipriya T, Fukuda N, Wang X, Fujimaki M. An angular fluidic channel for prism-free surface-plasmon-assisted fluorescence capturing. Nat Commun. 2013;4:1–7.
53. Krupka SS, Wiltschi B, Reuning U, Hölscher K, Hara M, Sinner EK. In vivo detection of membrane protein expression using surface plasmon enhanced fluorescence spectroscopy (SPFS). Biosens Bioelectron. 2006;22(2):260–7.
54. Toma M, Tawa K. Polydopamine thin films as protein linker layer for sensitive detection of interleukin-6 by surface plasmon enhanced fluorescence spectroscopy. ACS Appl Mater Interfaces. 2016;8(34):22032–8.
55. Sergelen K, Fossati S, Turupcu A, Oostenbrink C, Liedberg B, Knoll W, et al. Plasmon field-enhanced fluorescence energy transfer for hairpin aptamer assay readout. ACS Sensors. 2017;2(7):916–23.
56. Su X, Wu YJ, Robelek R, Knoll W. Surface plasmon resonance spectroscopy and quartz crystal microbalance study of streptavidin film structure effects on biotinylated DNA assembly and target DNA hybridization. Langmuir. 2005;21(1):348–53.
57. Laboratory methods for the diagnosis of *Vibrio cholerae*. Centers for Disease Control and Prevention (CDC); 2021. Available from: https://www.cdc.gov/cholera/pdf/laboratory-methods-for-the-diagnosis-of-vibrio-cholerae-chapter-7.pdf
58. Jawetz E, Melnick JL, Adelberg EA. Review of medical microbiology. 15th ed. Los Altos, CA: Lange Medical Publication; 1982. p. 227.
59. Loyprasert S, Hedström M, Thavarungkul P, Kanatharana P, Mattiasson B. Sub-attomolar detection of cholera toxin using a label-free capacitive immunosensor. Biosens Bioelectron. 2010;25:1977–83.
60. Viswanathan S, Wu LC, Huang MR, Ho JAA. Electrochemical immunosensor for cholera toxin using liposomes and poly(3,4-ethylenedioxythiophene)-coated carbon nanotubes. Anal Chem. 2006;78(4):1115–21.
61. Alfonta L, Willner I, Throckmorton DJ, Singh AK. Electrochemical and quartz crystal microbalance detection of the cholera toxin employing horseradish peroxidase and GM1-functionalized liposomes. Anal Chem. 2001;73:5287–95.
62. Karapetis S, Nikoleli GP, Siontorou CG, Nikolelis DP, Tzamtzis N, Psaroudakis N. Development of an electrochemical biosensor for the rapid detection of cholera toxin based on air stable lipid films with incorporated ganglioside GM1 using graphene electrodes. Electroanalysis. 2016;28(7):1584–90.
63. Song X, Shi J, Swanson B. Flow cytometry-based biosensor for detection of multivalent proteins. Anal Biochem. 2000;284:35–41.
64. Chen H, Hu QY, Zheng Y, Jiang JH, Shen GL, Yu RQ. Construction of supported lipid membrane modified piezoelectric biosensor for sensitive assay of cholera toxin based on surface-agglutination of ganglioside-bearing liposomes. Anal Chim Acta. 2009;657(2):204–9.

65. Kim CS, Seo JH, Cha HJ. Functional interaction analysis of GM1-related carbohydrates and vibrio cholerae toxins using carbohydrate microarray. Anal Chem. 2012;84:6884–90.
66. Phillips KS, Han JH, Martinez M, Wang Z, Carter D, Cheng Q. Nanoscale glassification of gold substrates for surface plasmon resonance analysis of protein toxins with supported lipid membranes. Anal Chem. 2006;78:596–603.
67. Zayats M, Raitman OA, Chegel VI, Kharitonov AB, Willner I. Probing antigen-antibody binding processes by impedance measurements on ion-sensitive field-effect transistor devices and complementary surface plasmon resonance analyses: development of cholera toxin sensors. Anal Chem. 2002;74(18):4763–73.
68. Kilian KA, Böcking T, Gaus K, King-Lacroix J, Gal M, Gooding JJ. Hybrid lipid bilayers in nanostructured silicon: a biomimetic mesoporous scaffold for optical detection of cholera toxin. Chem Commun (Camb). 2007;(19):1936–8. https://doi.org/10.1039/b702762a
69. Edwards KA, March JC. GM1-functionalized liposomes in a microtiter plate assay for cholera toxin in *Vibrio cholerae* culture samples. Anal Biochem. 2007;368(1):39–48.
70. Bunyakul N, Edwards KA, Promptmas C, Baeumner AJ. Cholera toxin subunit B detection in microfluidic devices. Anal Bioanal Chem. 2009;393(1):177–86.
71. Chiriacò MS, Primiceri E, D'Amone E, Ionescu RE, Rinaldi R, Maruccio G. EIS microfluidic chips for flow immunoassay and ultrasensitive cholera toxin detection. Lab Chip. 2011;4:658–63.
72. Archibald MM, Rizal B, Connolly T, Burns MJ, Naughton MJ, Chiles TC. A nanocoaxial-based electrochemical sensor for the detection of cholera toxin. Biosens Bioelectron. 2015;74:406–10.
73. Lim JM, Heo NS, Oh SY, Ryu MY, Seo JH, Park TJ, et al. Selection of affinity peptides for interference-free detection of cholera toxin. Biosens Bioelectron. 2018;99:289–95.
74. Achtsnicht S, Neuendorf C, Faßbender T, Nölke G, Offenhausser A, Krause HJ, et al. Sensitive and rapid detection of cholera toxin subunit B using magnetic frequency mixing detection. PLoS One. 2019:14(7):e0219356.
75. Bruzas I, Unser S, Yazdi S, Ringe E, Sagle L. Ultrasensitive plasmonic platform for label-free detection of membrane-associated species. Anal Chem. 2016;88(16):7968–74.
76. Schofield CL, Field RA, Russell DA. Glyconanoparticles for the colorimetric detection of cholera toxin. Anal Chem. 2007;79(4):1356–61.
77. Schmit VL, Martoglio R, Carron KT. Lab-on-a-bubble surface enhanced Raman indirect immunoassay for cholera. Anal Chem. 2012;84(9):4233–6.

SUPPORTING INFORMATION

Additional supporting information may be found online in the Supporting Information section at the end of the article.

How to cite this article: Seherler S, Bozdogan A, Ozal Ildeniz TA, Kok FN, Anac Sakir I. Detection of cholera toxin with surface plasmon field-enhanced fluorescent spectroscopy. Biotechnology and Applied Biochemistry. 2021;1–10. https://doi.org/10.1002/bab.2227